A Robust Differential-Amplitude Codification for Chipless RFID

Filippo Costa, *Member, IEEE*, Simone Genovesi, *Member, IEEE*, Agostino Monorchio, *Fellow, IEEE,* Giuliano Manara, *Fellow, IEEE*

***Abstract* — A novel robust encoding mechanism for spectral-domain chipless tags is proposed. The idea is based on storing information in a passive resonator by using a differential backscattering coding. This is achieved by subtracting multi-resonant slightly frequency-shifted amplitude responses obtained along vertical and horizontal polarization. The encoding mechanism is demonstrated by using a tag formed by a periodic surface patterned on a conductor-backed substrate. The unit cells of the periodic surface are formed by three concentric square loops loaded with asymmetric stubs. The resonant peaks are shifted finely and independently from each other by simply changing the length of the stubs. The reliability of the proposed encoding mechanism is experimentally verified by prototyping some samples of the tags on low-cost FR4 boards.**

***Index Terms*— Chipless RFID, Electromagnetic Absorbers, Frequency Selective Surfaces (FSS), Metamaterials, Radio Frequency Identification (RFID).**

I. Introduction

Barcode is today the most popular method of labeling objects even if it has significant limitations (short-range, non-automated tracking, operation in harsh environments, etc.). Many organizations are turning to Radio Frequency Identification (RFID) [1] but its application to consumer-packaged goods, postal items and books is feasible only if tag price goes under one cent. Despite significant investments, the price of tags is still not competitive when compared to barcodes because of the integrated circuit (IC) that poses a lower bound to the cost of tags. In the last few years efforts have been put in developing RFID tags with no ICs [2].

Two general types of chipless RFID tags can be identified: time domain (TD)-based and spectral (frequency) signature-based chipless RFID tags. Chipless tags of the first class encode information in time domain. The most promising configurations are surface acoustic wave (SAW) tags [3] and Thin Film Transistor Circuits (TFTCs) [4]. In the second class, bits are associated with the presence or absence of resonant peaks at a predetermined frequencies [5]–[10]. These tags are fully printable and extremely low cost but have limitations. The typical problems of available configurations are in terms of polarization sensitivity [5], [10], reading reliability and size, which is usually proportional to bits number. Being still in its infancy, chipless RFID technology needs further efforts to design high-capacity and reliable tags and sensors [11]. In general, the absence of a reference level for the backscattered signal makes the reading of chipless tags very complicate in realistic scenarios. Starting from this fundamental problem, a novel differential encoding mechanism is proposed. The tags here proposed respond with two frequency-shifted multi-resonant signals when interrogated with two orthogonal polarizations. The two responses are then subtracted to obtain very sharp frequency peaks. The tag configuration is based on a periodic surface [8] whose unit cell comprises a multi-loop resonator loaded with slightly different stubs along planar directions. To the best of our knowledge, it is the first time that polarization diversity [12] in chipless RFID has been used for making the codification more reliable.

[1]Manuscript received May, 2nd 2015.

The authors are with the Department of Information Engineering, University of Pisa, Via G. Caruso, 56122 - Pisa, Italy.e-mail: filippo.costa, (simone.genovesi, agostino.monorchio, g.manara)@iet.unipi.it

II. Differential-Backscattering Encoding mechanism and Chipless RFID Tag Configuration

In the conventional RFID technology, the decodification is facilitated by the fact that a change between two states is observed in the time domain with a fixed background scenario. However, in chipless RFID, this is not possible unless that the reader is fixed (*i.e.* a gate), since the tag is a completely passive structure. To partially solve this fundamental problem, it is here proposed to encode information in the difference between the responses along two orthogonal polarizations. The objective is to achieve a multi-resonant frequency response for the two orthogonal polarizations but slightly frequency-shifted. This allows to achieve very sharp peaks once that the curves are subtracted. The principle of operation of the device and the interrogation method are shown in Fig. 1. The adopted tag configuration, as shown in Fig. 2, consists of a periodic loop resonators patterned on the top of a conductor backed substrate. To achieve the desired frequency behaviour, a certain asymmetry has to be introduced in the resonators. The resonators are formed by three square loops loaded with stubs of different length along x and y directions. The presence of the ground plane at a suitable distance from the resonators guarantees the deep absorption peaks and independence of objects where the tag is placed on. The RCS value of the tag can be controlled with the number of the unit cells employed. The larger is the size of the structure, the larger is the RCS value [13]. The periodic structure can be quickly analysed by using a Periodic Method of Moment (PMM) [14], [15]. The length of the stubs is different along x and y directions in order to provide slightly different frequency responses for the two polarizations.

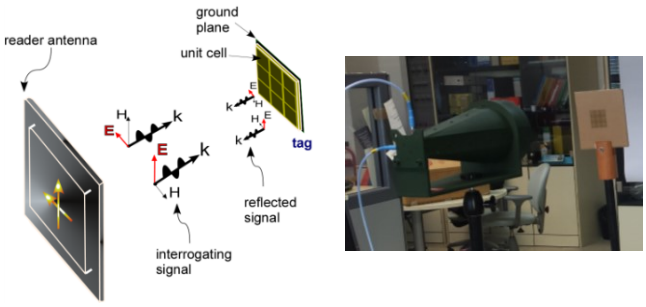

(a) *(b)*

Fig. 1– *(a)* Sketch of the interrogating mechanism of differential coded chipless tags. *(b)* Experimental setup.

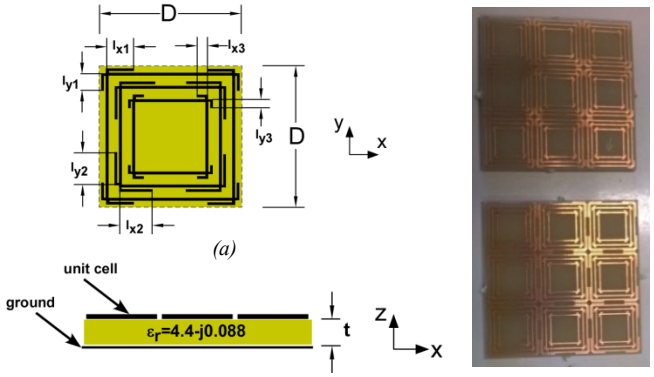

(a) *(b)* *(c)*

Fig. 2. *(a)* Unit cell geometry of the periodic surface-based chipless RFID, *(b)* side view of the proposed chipless tag, *(c)* chipless RFID prototypes.

The size of the unit cell and thus its periodicity D is equal to 15 mm. Every unit cell is discretized with a grid of 64x64 pixels to obtain tag design (the width of the loop and the stubs is one pixel, 1/64**D*=0.234 mm) which is well above the minimum precision of a standard photolithographic process (5 mills, that is around 0.13 mm). Absorption at the three resonance frequencies is achieved if the substrate losses and the thickness are suitably chosen [14]. In this case FR4 (ε_r=4.4- j0.088) with a thickness *t* of 1.6 mm is chosen. The thickness of the resonator can be further reduced to increase the Q factor and to adapt it to thinner objects. In the case of FR4 (high loss substrate) the substrate thickness can be reduced down to 0.6 mm or 0.8 mm but a further decrease leads to mismatch with free space impedance and therefore a reduced absorption [14]. However, if a substrate with a smaller amount of losses is employed (*e.g.* ε_r=4.4-j0.01) the substrate thickness can be reduced down to 0.2 mm. As an example, the reflection coefficient of an infinite periodic structure with the stubs along the *y*-direction set slightly longer than the *x*-directed stubs ($l_{yn} = l_{xn}+1$), is reported in Fig. 3a. The reflection coefficient is shown at normal incidence but it is extremely stable with respect to the elevation incidence angle [8]. By subtracting the reflected signals obtained with two simultaneous interrogations of the tag, well visible spikes in correspondence of each resonance frequency are obtained (Fig. 3b). The number of employed loops is directly proportional to the number of encoded bits. In order to avoid undesired coupling effects among loops, only three loops are employed and a hybrid coding scheme based on frequency shift is exploited [6].

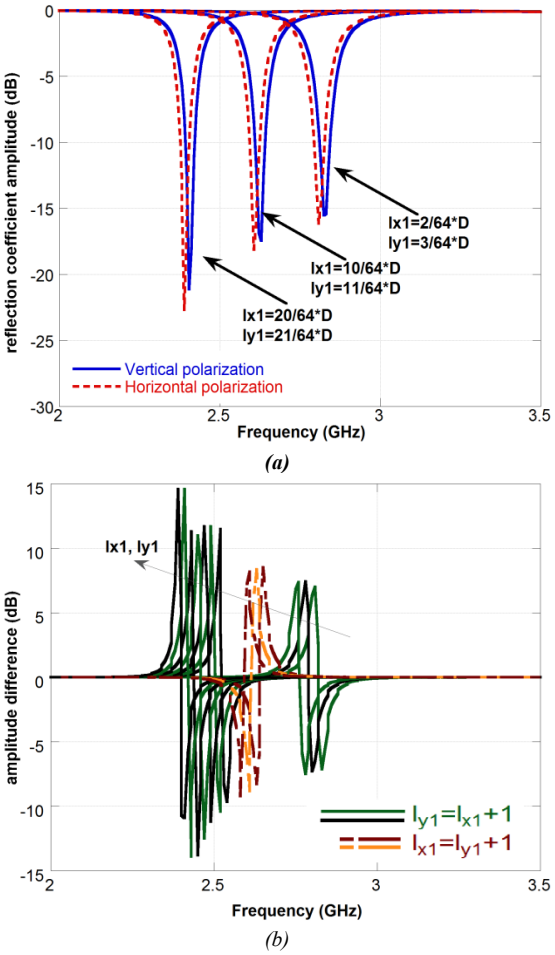

Fig. 3. *(a)* Amplitude of reflection coefficient for vertical and horizontal polarizations of an infinite array of 3-loop with stubs. *(b)* Amplitude difference between the reflection coefficients. The curves are obtained by progressively varying the length of the *x* and *y* directed stubs of the first loop and imposing $l_{y1} = l_{x1}+1$ or $l_{x1} = l_{y1}+1$. The other stubs are fixed as: $l_{x2} = l_{x3} = 2/64$ D, $l_{y2} = l_{y3} = 4/64$ D.

This means that the codification is not binary but the base is equal to the number of different conditions that the resonant peaks can assume. For instance, the stubs of the first loop can be varied from 2 to 31 pixels leading to 30 different conditions. Moreover, additional 30 conditions are obtained by using the inverse coding obtainable by imposing the *x*-directed stub slightly longer than *y*-directed stub (dashed curves in Fig. 3b). It is important to highlight that the shift of the first resonant peak does not lead to any variation of the other two resonant peaks thus guarantying the robustness of the encoding mechanism. Similar behaviours are obtained for the second and the third loops. The quantity of information stored in the tag can be calculated as follows:

$$Nbit = \log_2(N_{s1}) + \log_2(N_{s2}) + \log_2(N_{s3}) \qquad (1)$$

where N_{s1}, N_{s2} and N_{s3} are the number of possible states associated to the first, the second and the third loop, respectively. In our case, $N_{s1} = 60$, $N_{s2} = 38$, $N_{s3} = 26$ and *Nbit*=15.86. Each frequency peak occupies a bandwidth of roughly 0.4% leading to an efficient exploitation of the spectrum.

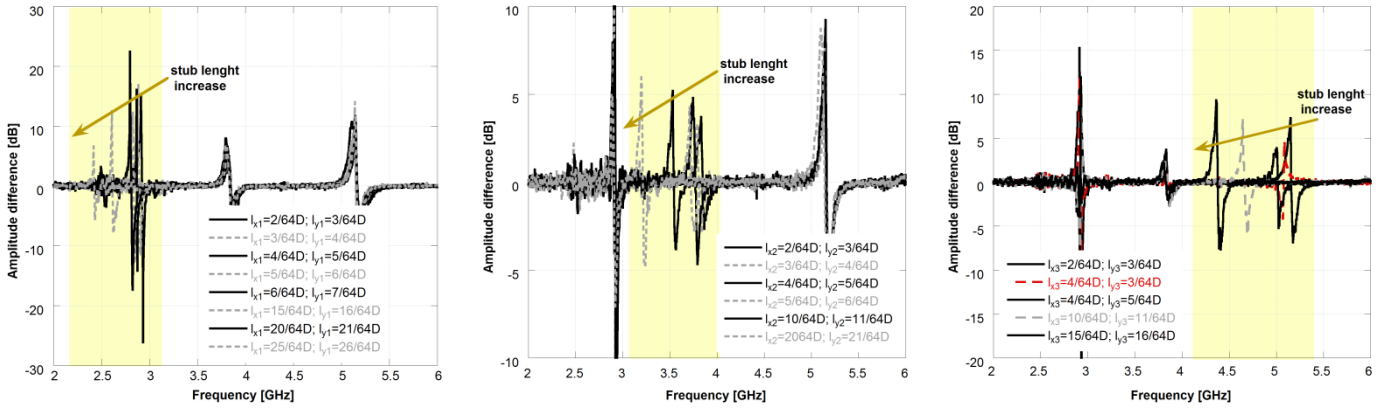

(a) *(b)* *(c)*

Fig. 4 – *(a)* Measured amplitude difference for eight different bit sequences obtained by progressively varying the length of the stubs of the first loop and imposing $l_{y1}=l_{x1}+1$. The other stubs are fixed at the lowest length: $l_{x2}=l_{x3}=2/64D$, $l_{y2}=l_{y3}=3/64D$. *(b)* Varying the length of the stubs of the second loop with $l_{y2}=l_{x2}+1$ and the other stubs fixed at the lowest length: $l_{x1}=l_{x3}=2/64D$, $l_{y1}=l_{y3}=3/64D$. *(c)* varying the length of the stubs of the third loop with $l_{y3}=l_{x3}+1$ or $l_{x3}=l_{y3}+1$ and the other stubs fixed at the lowest length: $l_{x1}=l_{x2}=2/64D$, $l_{y1}=l_{y2}=3/64D$.

III. Experimental Results

Some prototypes having the same characteristics of the simulated ones have been manufactured on FR4 substrate (Fig. 3c) by truncating the periodic surface to a few unit cells. The number of unit cells employed determines the average value of Radar Cross Section (RCS) and therefore the read range [13]. Measurements have been performed by using an Agilent E5071C vector network analyzer in a non-anechoic environment with a level of transmitted power equal to 0 dBm. A dual-polarized wideband horn antenna (Flann DP280) is used as reference antenna. The setup was shown in Fig.1b. Measurements were carried out for vertical and horizontal polarization and the S_{11} and S_{22} are stored simultaneously. A normalization procedure which combines three measurements (tag, ground plane of the same size of the tag and background) [8] was used to remove undesired effects do to multipath and reader antenna coupling. The differential encoded signals, for several encoding states, obtained by subtracting the vertical and horizontal polarizations signals, are illustrated in Fig. 4. More in detail, the differential reflection coefficient for different stub lengths, varying progressively from the minimum to the maximum length, is reported for each of the three loops. It is worth underlying that the resonance frequency of each resonant loop is not subject to any variation when the length of stubs belonging to the other loops are changed. The performance of the tag are quite stable even in non-line of sight since the scattering pattern of the resonator is not directive.

IV. Conclusion

A novel robust encoding mechanism relying on polarization diversity has been presented. A differential multi-frequency spectral response has been obtained by subtracting the two responses of a tag obtained through an interrogation with a dual polarized antenna. The employed resonators comprise three concentric loops loaded with stubs of different lengths along the two main planar directions. The new encoding approach is presented and experimentally verified demonstrating a reliable 16 bits tag.

V. References

[1] K. Finkenzeller and R. Waddington, *RFID handbook: radio-frequency identification fundamentals and applications*. Wiley New York, 1999.

[2] S. Preradovic and N. C. Karmakar, "Chipless RFID: Bar Code of the Future," *IEEE Microwave Magazine*, vol. 11, no. 7, pp. 87–97, Dec. 2010.

[3] V. P. Plessky and L. M. Reindl, "Review on SAW RFID tags," *IEEE Transactions on Ultrasonics, Ferroelectrics and Frequency Control*, vol. 57, no. 3, pp. 654–668, Mar. 2010.

[4] R. Das and P. Harrop, "RFID forecasts, players and opportunities 2009–2019," *IdTechEx report*, 2009.

[5] B. Shao, Q. Chen, Y. Amin, R. Liu, and L.-R. Zheng, "Chipless RFID tags fabricated by fully printing of metallic inks," *Ann. Telecommun.*, vol. 68, no. 7–8, pp. 401–413, Aug. 2013.

[6] A. Vena, E. Perret, and S. Tedjini, "Chipless RFID Tag Using Hybrid Coding Technique," *IEEE Transactions on Microwave Theory and Techniques*, vol. 59, no. 12, pp. 3356–3364, Dec. 2011.

[7] S. Preradovic, I. Balbin, N. C. Karmakar, and G. F. Swiegers, "Multiresonator-Based Chipless RFID System for Low-Cost Item Tracking," *IEEE Transactions on Microwave Theory and Techniques*, vol. 57, no. 5, pp. 1411–1419, May 2009.

[8] F. Costa, S. Genovesi, and A. Monorchio, "A Chipless RFID Based on Multiresonant High-Impedance Surfaces," *Microwave Theory and Techniques, IEEE Transactions on*, vol. 61, no. 1, pp. 146–153, 2013.

[9] C. M. Nijas, U. Deepak, P. V. Vinesh, R. Sujith, S. Mridula, K. Vasudevan, and P. Mohanan, "Low-Cost Multiple-Bit Encoded Chipless RFID Tag Using Stepped Impedance Resonator," *IEEE Transactions on Antennas and Propagation*, vol. 62, no. 9, pp. 4762–4770, Sep. 2014.

[10] A. Blischak and M. Manteghi, "Embedded Singularity Chipless RFID Tags," *IEEE Transactions on Antennas and Propagation*, vol. 59, no. 11, pp. 3961–3968, Nov. 2011.

[11] D. Girbau, A. Ramos, A. Lazaro, S. Rima, and R. Villarino, "Passive Wireless Temperature Sensor Based on Time-Coded UWB Chipless RFID Tags," *IEEE Transactions on Microwave Theory and Techniques*, vol. 60, no. 11, pp. 3623–3632, Nov. 2012.

[12] A. Vena, E. Perret, and S. Tedjini, "A compact chipless RFID tag using polarization diversity for encoding and sensing," in *2012 IEEE International Conference on RFID (RFID)*, 2012, pp. 191–197.

[13] F. Costa, S. Genovesi, and A. Monorchio, "Chipless RFIDs for Metallic Objects by Using Cross Polarization Encoding," *IEEE Transactions on Antennas and Propagation*, vol. 62, no. 8, pp. 4402–4407, Aug. 2014.

[14] F. Costa, S. Genovesi, A. Monorchio, and G. Manara, "A circuit-based model for the interpretation of perfect metamaterial absorbers," *IEEE Transactions on Antennas and Propagation*, vol. 61, no. 3, pp. 1201–1209, 2013.

[15] F. Costa, A. Monorchio, and G. Manara, "An equivalent-circuit modeling of high impedance surfaces employing arbitrarily shaped FSS," in *Electromagnetics in Advanced Applications, 2009. ICEAA'09. International Conference on*, 2009, pp. 852–855.